

CONTROL OF THE INTERFERENCE FRINGES IN A POINT DIFFRACTION INTERFEROMETER USING AN OPTICAL SATURABLE ABSORBER

Hideo Furuhashi¹, Yoshiyuki Uchida¹, Kiyofumi Matsuda² and Akihiro Kono³

¹Department of Electrical and Electronics Engineering
Aichi Institute of Technology

1247, Yachigusa, Yakusa-cho, Toyota, 470-0392 Japan

²Graduate School for the Creation of New Photonics Industries, Japan

³Graduate School of Engineering, Nagoya University, Japan

INTRODUCTION

A point diffraction interferometer (PDI) is a common-path interferometer that can be used to easily measure either the variation in the phase across a wavefront or the change in the refractive index of a transparent phase object [1-4]. Point-diffraction interferometers have a simple construction and are inherently stable. Thus they are useful for testing and evaluating optical elements, and analyzing phase objects, fluid flow diagnostics, for example. However, the filter in a PDI has an extremely small dot, and it is difficult to focus the wavefront on such a small dot. Therefore, we have proposed a PDI that employs an optical saturable absorber. In this system, the small dot is generated automatically on the film and the focal point is self-aligned. One disadvantage of this system, however, is that the fringe contrast decreases over a long period of time. We have demonstrated that this problem can be overcome by stabilizing the fringe pattern by applying blue light [5].

It is difficult to vary the transparency of the film in a conventional PDI, making it impossible to control or optimize the fringe contrast, since the contrast depends on the light intensity passing through the PDI dot. However, the technique using blue light has the advantage that the characteristics of the filter (the transparency and the size of the dot) can be adjusted, so that the maximum contrast can be obtained.

In this paper, the control of the fringe pattern contrast in a PDI using an optical saturable absorber and blue light is discussed in detail.

THEORY

Figure 1 shows a schematic diagram of a conventional PDI system. A transparent dot filter is employed in a conventional PDI system. A

wavefront in the object plane is focused on the filter using a Fourier-transform lens. The interference image is observed in the image plane. The optical image intensity is given by [5]

$$I = A^2 \left\{ \alpha^2 + \gamma^2 \cdot (\alpha_{foc} - \alpha)^2 + 2 \cdot \alpha \cdot \gamma (\alpha_{foc} - \alpha) \cdot \cos[i\phi(x, y)] \right\} \quad (1)$$

Here, A and $i\phi(x, y)$ are the absolute amplitude and phase of the wavefront in the object plane respectively, x and y are orthogonal coordinates, α and α_{foc} are the amplitude transmittances of the filter outside and inside the dot respectively, and γ is the ratio of the light passing through the PDI dot.

The fringe contrast is defined as

$$V = \left| \frac{2 \cdot \alpha \cdot \gamma \cdot (\alpha_{foc} - \alpha)}{\alpha^2 + \gamma^2 \cdot (\alpha_{foc} - \alpha)^2} \right| \quad (2)$$

Therefore, the contrast changes with γ . It has a maximum value of 1 when

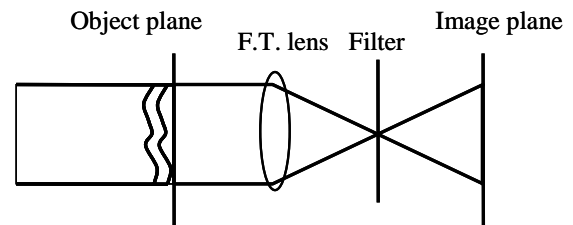


FIGURE 1. Schematic diagram of a PDI system. F.T. lens: (Fourier transform lens)

$$\gamma = \left| \frac{\alpha}{\alpha_{foc} - \alpha} \right|. \quad (3)$$

It is difficult to vary the transparency of the film in a conventional PDI.

Figure 2 shows the experimental set-up of a PDI that employs a saturable absorber. A saturable absorber, photochromic bacteriorhodopsin (BR) film, is used as the filter. Figure 3 shows a schematic diagram of a simplified photocycle of a BR film. BR568 is the ground state, while M412 is the excited state. The film absorbs light having wavelengths between 500 and 700 nm by the excitation of molecules in the ground state to the excited state. It has a very high resolution of over 5000 lines/mm and a low saturation energy. It has a relaxation time, (defined as the time taken for 63% (1/e) of all excited state molecules to return to the ground state) of 40-80 s at a temperature of 22°C.

If a wavefront from a collimated laser, which has an output wavelength in the range 500-700 nm, passes through a transparent phase object and is focused on the film, the point becomes transparent. Thus, the BR-film acts as a PDI filter. The film has a maximum absorption at 568 nm, therefore He-Ne lasers having output wavelengths of 633 nm and 543.5 nm were used in this experiment. We then applied blue light from a xenon lamp, which de-excites the M412 state to the BR568 ground state. The film absorbs light with a wavelength below 500 nm by de-excitation.

The absorption rate of the film is given by [5]

$$\beta_{abs} = k_{12} \cdot \frac{N_0}{I' \cdot k_{12} + I'' \cdot k_{21}} [I'' \cdot k_{21} + I' \cdot k_{12} \cdot \exp\{-(I' \cdot k_{12} + I'' \cdot k_{21})t\}] + \beta_0 \quad (4)$$

Here, k_{12} and k_{21} are the absorption coefficients for the excitation light in the ground state and for the de-excitation light in the excited state respectively, N_0 is the molecular surface density, β_0 is the background absorption rate of the film, and I' and I'' are the optical intensities of the excitation light and the de-excitation light at the film, respectively. After a long time, it becomes

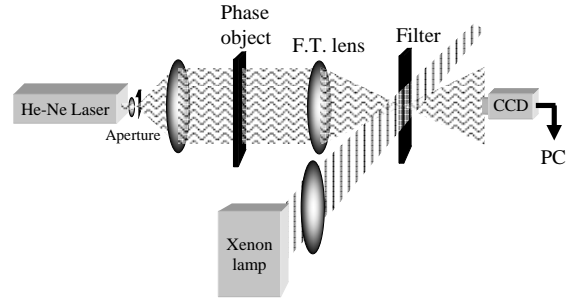


FIGURE 2. Experimental set-up of a point diffraction interferometer using a saturable absorber, He-Ne laser and blue light.

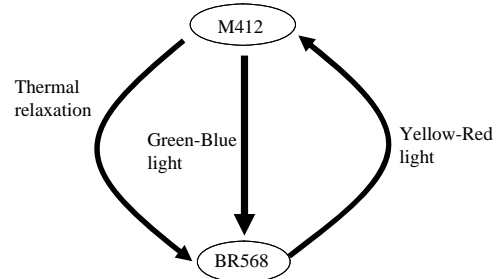


FIGURE 3. Schematic diagram for a simplified photocycle of the BR film.

$$\beta_{abs} = N_0 \cdot k_{12} \frac{1}{1 + \frac{I'}{I''} \cdot \frac{k_{12}}{k_{21}}} + \beta_0. \quad (5)$$

If the excitation light intensity I' is very high, the absorption becomes small.

The absorbencies for the ground-state film and excited-state film used in this experiment are 2 and 0.7 for the 633-nm-wavelength radiation of the He-Ne laser, respectively. Those for 543.5 nm are 6 and 0.9, respectively. Therefore, $N_0 \cdot k_{12} = 1.3$ and $\beta_0 = 0.7$ for the 633-nm-wavelength He-Ne laser. $N_0 \cdot k_{12} = 5.1$ and $\beta_0 = 0.9$ for the 543.5-nm-wavelength He-Ne laser.

The amplitude transmittances α of the filter outside the focal point are 0.37 and 0.05 for wavelengths of 633 nm and 543.5 nm, respectively. The saturated amplitude transmittances are 0.7 and 0.64 for the

wavelengths of 633 nm and 534.5 nm, respectively. Figure 4 shows the fringe contrast calculated using equation (2). Figure 4(a) is for the 633-nm laser while Fig. 4(b) is for the 534.5-nm laser.

Since the amplitude transmittance inside the focal point is larger than that outside the focal point, maximum contrast is obtained when $\alpha_{foc} = \left(1 + \frac{1}{\gamma}\right)\alpha$. However, the maximum amplitude transmittances α_{foc} of the filter inside

the focal point are 0.7 and 0.64 for 633 nm and 534.5 nm, respectively. Therefore, maximum contrast is obtained at the maximum α_{foc} of 0.7 for the 633-nm-wavelength laser having a wavelength of 633 nm. It is smaller than 1. On the other hand, a maximum contrast of 1 is obtained by controlling the transmittance α_{foc} between 0.05 to 0.64 for the 534.5-nm-wavelength laser.

In general, the necessary condition for obtaining a fringe contrast of 1 is

$$\frac{\alpha|_{\max}}{\alpha} > 1 + \frac{1}{\gamma}. \quad (6)$$

Here, $\alpha|_{\max}$ is the saturated amplitude transmittance of the film. This condition can be written as follows in terms of the absorbance of ground state b_{BR} and that of the excited state b_M for the exciting light.

$$\exp\left(\frac{b_{BR} - b_M}{2}\right) > 1 + \frac{1}{\gamma} \quad (7)$$

Therefore, the 534.5-nm-wavelength laser gives good contrast. However, the large absorption of BR state at this wavelength results in a low intensity of the fringe. Therefore, if $\gamma \approx 1$, the 633-nm-wavelength He-Ne laser is the most suitable for measuring the fringes for the BR film used in this experiment. Better fringe contrast is obtained by using a thinner film for the 534.5-nm-wavelength laser.

Next we consider the focused plane wave which has an optical intensity profile on the focal point given by

$$I'_{plane} = I_p \left\{ \frac{2J_1\left(\frac{a}{\lambda \cdot f} r\right)}{\frac{a}{\lambda \cdot f} r} \right\}^2. \quad (8)$$

Here, I_p is the peak intensity at the focal point, f and a are the focal length and radius of the Fourier-transform lens, respectively. The

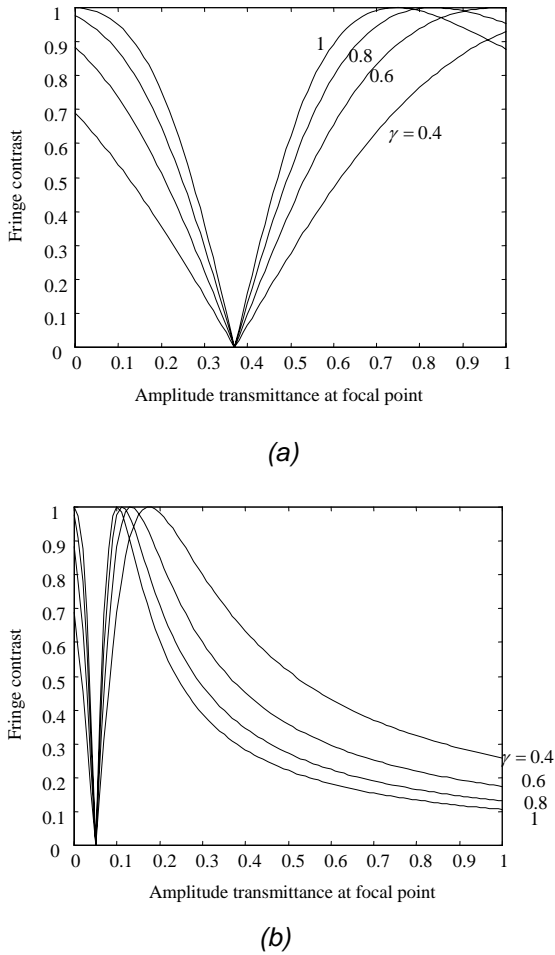


FIGURE 4. Relationships between fringe contrast and amplitude transmittance at the focal point for the (a) 633-nm-wavelength and (b) 534.5-nm-wavelength He-Ne laser.

amplitude transmittance profile is given as follows.

$$\alpha_{foc}(r) = \exp \left(-\frac{N_0 \cdot k_{12}}{2} \frac{1}{1 + \frac{I'_{plane} \cdot k_{12}}{I'' \cdot k_{21}}} - \frac{\beta_0}{2} \right) \quad (9)$$

Figure 5 shows the amplitude transmittance of plane wave calculated by using equations (8) and (9). The transmittance can be changed by changing the intensity of the de-excitation light. The PDI dot size can be also changed. Therefore, the contrast can be controlled by varying the intensity of the de-excitation light.

CONCLUSIONS

In conclusion, control of the contrast of the fringe pattern in a PDI using an optical saturable absorber and blue light has been discussed in detail. The contrast can be varied by the adjusting the intensity of the blue light. Therefore, it is possible to obtain good contrast for a wide variety of wavefronts by using this method.

REFERENCES

1. R. N. Smart, Jpn. 1975, Theory and application of point-diffraction interferometers, J. Appl. Phys. Suppl. 14: 351-356.
2. C. P. Grover, 1975, Random partial diffuser as beam splitter in a new, common path interferometer, Opt. Commun, 13: 335-337.
3. R. N. Smart, 1979, Special applications of the point diffraction interferometer, Proc. SPIE, 192: 35-40.
4. Hideo Furuhashi, Atsushi Shibata, Yoshiyuki Uchida, Kiyofumi Matsuda and Chander P. Grover, 2004, A Point diffraction interferometer with random-dot filter, Opt. Commun. 237, 17-24.
5. Hideo Furuhashi, Atsushi Shibata, Yoshiyuki Uchida, Kiyofumi Matsuda and Chander P. Grover, 2004, Point diffraction interferometer using an optical saturable absorber, Proc. 9th Annual ASPE Meeting.

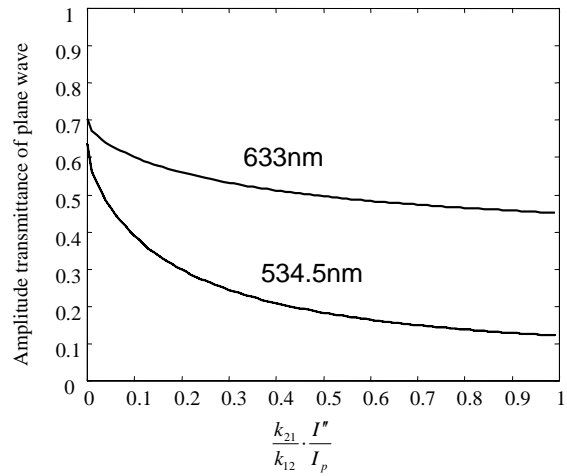


FIGURE 5. Calculated amplitude transmittance profile applied He-Ne laser. (a) 633 nm, (b) 543.5 nm